WING DESIGN OF SUPERSONIC TRANSPORT BY A MULTI-POINT OPTIMIZATION METHOD

Kentaro HIGUCHI*, Zhong LEI and Kenichi RINOIE***
***Department of Aeronautics and Astronautics, The University of Tokyo, Tokyo, 113-8656, JAPAN**
****Aviation Program Group, Japan Aerospace Exploration Agency, Tokyo, 181-0015, JAPAN**

Keywords: *Supersonic Transport, Multi-Point Optimization, Low Fidelity Method*

Abstract

One of the difficulties in the aerodynamic design of a supersonic transport is the wing design considering both supersonic and low-speed performance. The wing with large sweepback angle and low aspect ratio is often used to reduce wave drag at supersonic cruise, but it also results in poor performance at low speeds such as take-off and landing conditions. Therefore, a large area is required for the wing to generate enough lift and, consequently reduce the take-off and landing field length. On the other hand, this also leads to an increase in aircraft weight and uneconomical flight. The purpose of this research is to propose a multi-point design method which can obtain a compromised solution of wings for a supersonic transport, by using low fidelity methods such as a combination of the Quasi-Vortex-Lattice Method and the Leading-edge Suction Analogy for high-lift device design at low-speeds, and the supersonic linear theory at supersonic speeds. The multi-point design method proposed in this paper is applied to a conceptual design of a supersonic regional jet. Results show that the multi-point design can improve aircraft performance by reducing the wing area and thus the aircraft weight, and suggests a guideline towards the optimization of wings in the conceptual design phases.

Nomenclature

AR	wing aspect ratio
C_D	drag coefficient
C_{Di}	induced drag coefficient
C_L	lift coefficient
I_x	moment of inertia, m^4
I_P	polar moment of inertia, m^4
L/D	lift-to-drag ratio
M_x	bending moment, Nm
M_y	twisting moment, Nm
S_W	wing area, ft^2
T/W	thrust-to-weight ratio
W_{TO}	maximum take-off weight, lb
x	chordwise coordinate measured from the aircraft nose, ft
x_W	chordwise coordinate measured from the wing apex, ft
y	spanwise coordinate orthogonal to x, measured from the wing center-line, ft
z	coordinate orthogonal to the x-y plane, ft
α	angle of attack, degree
δ	flap deflection angle, degree

Subscripts

le	leading-edge
te	trailing-edge

1 Introduction

Recently, there is a high interest in the next generation Supersonic Transport (SST). Researches to make the next generation supersonic transport (SST) a reality are being carried out all over the world. The supersonic business aircraft concept has been studied [1, 2] and the HISAC project[1] lead by Dassault Aviation, focuses on noise reduction and NOx emission. In Japan, the former National Aerospace Laboratory of Japan (NAL) which is

now the Japan Aerospace Exploration Agency (JAXA) successfully launched a scaled supersonic experimental airplane in Australia in 2005[4], and validated computational design methods as well as retrieving flight data. Presently, JAXA is promoting the Silent Supersonic Technology Demonstrator (S^3TD) project[5] which puts emphasis on low sonic boom, noise reduction, and integration of advanced demonstration system.

One of the factors which make the aerodynamic design of the SST difficult is the wing aerodynamic design. Usually, to reduce wave drag at supersonic cruise, wings with highly-swept leading edge and low aspect ratio wing are adopted. However, this type of wing is known to have poor aerodynamic performance at low speeds and can possibly put the designers into the following cycle. The wing area will have to be large enough to generate lift for take-off and landing within the required runway length. In the meantime, a large wing area associates with large additional profile drag and wave drag at cruise conditions, and inevitably make worsen the cruise performance; bad cruise performance consumes more fuel, thus increase weight; in turn, the increased fuel requires a larger wing area. On the other hand, improvement of the aerodynamic performance and reduction of weight can reduce engine power setting and therefore community noise. So, to avoid this problem in the design of a wing for the SST, it is desirable to use a multi-point design method which takes into account both supersonic and low speed performance. Compared with high fidelity methods, such as computational fluid dynamics which is used currently in many aerodynamic designs with large computational cost, a low fidelity method will be useful for multi-point design and conceptual design phases where large numbers of calculation cases are required. Therefore the objective of this study is to develop a tool to design wings for the SST considering both supersonic and low speed performance.

This study combines optimization of wing planform at supersonic cruise conditions with high-lift device design at low-speeds, and is intended to investigate possibility of a wing which has less weight, better aerodynamic performance at both supersonic cruise condition and take-off / landing and satisfies structure constraints. For the optimization of wing planform at supersonic cruise condition, estimation of aerodynamic performance and structural analysis are integrated in an automatic design process, which is driven by genetic algorithm methods implanted in a commercially-available software iSIGHT-FD (Engenious Software Inc.). Also, low fidelity methods are used to reduce computational cost, which will be useful when considering preliminary design where many cases or configurations must be put into consideration.

In this paper, the calculation methods for low speed and supersonic flight conditions will be described. The Quasi-Vortex-Lattice Method [6] coupled with the Leading-Edge Suction Analogy [7] (QVLM-SA) will be used as the calculation method for low speed aerodynamics, and a Supersonic Linear Theory (SLT) proposed by Carlson [8] will be employed for calculations at supersonic cruise conditions. Some numerical tests using QVLM-SA will be conducted and compared with corresponding wind-tunnel experiments to validate the method. Results show that QVLM-SA can well estimate the qualitative effects of flaps. Since, the supersonic linear theory (SLT) has been used to design the scaled supersonic experimental airplane at the National Aerospace Laboratory of Japan, it can be said that the applicability is already validated. Furthermore, as an example, the multi-point design method will be applied to the conceptual design of a supersonic regional jet (SSRJ).

2 Analytical Methodology

2.1 Calculation Method for Low-Speed Aerodynamics

The method for low-speed aerodynamic calculation was developed by coupling the classical Quasi-Vortex-Lattice Method (QVLM) with the Leading-Edge Suction Analogy (LESA). In this paper, this method is called QVLM-SA[9]. Wings with large leading-edge sweep angles used for a SST are known to form leading-edge separation vortices, which

generate additional lift and drag. LESA is a simple method to estimate the vortex forces, by assuming that the amount of vortex suction acting normally on the wing surface is equal to the amount of leading-edge suction acting normally on the leading-edge to the upper surface. The potential forces are calculated by QVLM which divides the wing into trapezoidal or triangular regions, and distributes vortex segments and control points for each region. The vortex suction forces are calculated using the leading-edge suction calculated in the process by LESA. Details of the QVLM-SA calculation are described in [9].

2.2 Calculation Method for Supersonic Aerodynamics

The Supersonic Linear Theory (SLT) was employed to calculate supersonic aerodynamics. Wing camber and twist (warp) are designed to reduce the lift-induced-drag by Carlson's method[8] based on the SLT. Although the SLT is a low fidelity method, its capability has been verified in the past. Also SLT has been applied in the aerodynamic design of the scaled supersonic experimental (NEXST)[10] and the usability of the method has been confirmed.

2.3 The Optimization of Wing Planform

The above SLT was used with a commercially available optimization software iSIGHT-FD to optimize the wing planform at supersonic speeds. NCGA (Neighbor Cultivation Genetic Algorithm) embedded inside iSIGHT-FD was used for multi-objective optimization by setting several objective functions in the design process. Minimization of induced drag will be the primary objective of wing planform optimization. However without the constraint of structural considerations, it is known that a wing planform with a large aspect ratio has better aerodynamic performance. To obtain realistic solutions, the pressure distribution calculated by SLT was integrated on the wing to calculate the bending and twisting moments (around the quarter location of the mean aerodynamic chord), which were taken as other objectives in the optimization. The bending moment and twisting moment acting on wing cross sections were obtained by integrating the aerodynamic load and the weight of wing structure [11]. The wing weight was estimated by [12]. To account for the rigidity of the wing section, the bending moment was divided by the moment of inertia of cross-sectional area I_x, and the twisting moment was divided by the polar moment of inertia of cross-sectional area I_P.

2.4 A Multi-Point Design Method

The flow of the multi-point design of SST wings is shown in Fig. 1. In the first phase, the wing planform will be optimized using iSIGHT-FD. Each planform is warped by the Carlson's method to minimize the induced drag at a specified lift coefficient. Then, the fuselage and the tail are designed as will be explained in section 4.2.3. Afterwards, the high-lift devices will be designed at a low speed condition by the use of QVLM-SA. It will now be possible to evaluate the take-off and landing performance. If the take-off and landing performances (see section 4.2.4) meet the requirements, it will be considered whether the wing area can be reduced for weight reduction. In the second phase, the wing planform with the modified wing area will be re-optimized, and the design process will repeated, until the take-off and landing performance is fulfilled.

It must be noted that, the weight and parasite drag are estimated by empirical methods used in traditional conceptual design [12, 13], and the accuracy is generally not very accurate. Therefore, in this study, we just intend to analyze the design and provide useful information for the wing at the preliminary design phase.

3 Verification of the Calculation Methods

3.1 QVLM-SA

To verify the applicability of QVLM-SA, calculation was compared with a wind tunnel test conducted at the former National Aerospace Laboratory of Japan (presently JAXA)[14]. The geometry of the wind tunnel test model is shown in Fig. 2. The model consists of a cranked- arrow wing planform, an

axisymmetrical body, inboard and outboard leading-edge flaps (LEF), and trailing-edge flaps (TEF). The camber and twist of the main wing was designed by Carlson's method based on the supersonic linear theory. Measurements were carried out for various flap deflection combinations. For simplicity, the flap deflection configurations will be named Sxxyyzz, where "xx", "yy", and "zz" represent the inboard LEF, outboard LEF, and the TEF, respectively. Details of the wing model are described in [15]. The Reynold's number based on the wing's mean aerodynamic chord was 9.45×10^5.

Figure 3. compares lift coefficient C_L and drag coefficient C_D of the experimental and the computational results for configurations S00000, S000010, S301200, and S301210. An empirical method suggested in [16] was used to estimate fuselage aerodynamic characteristics. To account for the skin friction drag, the minimum drag calculated from the experimental results of the baseline S000000 configuration was added to the drag coefficients in all calculations. Also, since the main wing has a warped wing section, the C_L at α=0° will not be zero. Therefore the angles of attack in the calculation were offset by 1° according to the experiment. It can be seen that experiment and calculation well agree with each other up to a moderate angle of attack of 10°. However, discrepancy can be seen at high angles of attack due to vortex breakdown observed in the experiment. The non-linear effect due to vortex breakdown cannot be simulated by QVLM-SA.

To investigate effect of flap on the aerodynamic performance, the lift and drag increment (ΔC_L, ΔC_D) compared to the baseline S000000 configuration was calculated. Fig. 4. shows the ΔC_L-α and ΔC_D-α curves of the experiment and calculation. Though the calculation results do not agree exactly with the experiment, the overall patterns of the results are generally well reproduced. So it can be said that QVLM-SA can estimate the qualitative effects of flap.

Furthermore, validation was carried out for other wind tunnel tests conducted at NASA [17, 18], to verify that QVLM-SA can be applied to various types of wing planforms. Reference [17] tested a highly swept arrow wing with segmented leading- and trailing edge flaps at Mach number of 0.25. Reference 18 investigated 70°/49° cranked arrow wing with leading- and trailing flaps at Mach number of 0.205. Comparison of experiment and calculation show that, at low angles of attack, the calculation results agree well with experiment for configurations with and without flap deflection (Fig. 5). The qualitative flap effects were also well estimated when leading- and trailing-edge flaps are deflected differently (Fig. 6). Therefore, it can be concluded that QVLM-SA is capable of estimating aerodynamic forces for arbitrary wing and flap planform.

3.2 Supersonic Linear Theory (SLT)

Carlson's warp design method can be used to reduce lift-induced drag at supersonic speeds. Some preliminary calculations were tested using iSIGHT-FD. The optimization method used is Multi-Island Genetic Algorithm (MIGA), and a parametric study was carried out using the 20,000 individuals calculated during the optimization. Seven design parameters which define the wing planform are shown in Fig. 7. The calculation conditions are as follows.

- M1.6
- S_W=1,883 ft^2
- Design cruise C_L = 0.1
- Number of islands 15
- Number of individuals per island 15
- Number of generations 100

The wing area and design C_L was set referring to the supersonic regional jet proposed at JAXA, which will be introduced later.

Figure 8 shows some preliminary calculation results. This figure shows induced drag versus bending moment (Fig.8(a)) and induced drag versus twisting moment (Fig.8(b)) for different wing aspect ratios *AR*. In Fig. 8(a), the calculated individuals are scattered in a graph with the induced drag as the vertical axis and the bending moment as the horizontal axis. In Fig. 8(b), the twisting moment is used as the horizontal axis. It can be observed from the graphs that there is a tradeoff between aerodynamic and structural characteristics in front of the solutions. When the wing has an

aerodynamic advantage (small drag), the structural load will become large.

4 A Design Example of a Supersonic Regional Jet

4.1 The Baseline

The reduction of sonic boom is one of the most important problems for SST research. It is very difficult to reduce the level of sonic boom to an acceptable value by current technology due to the large payload and range of the SST. Therefore, a suitable goal for the present SST technology may be considered as a small scale aircraft with less weight and less challenging from a low-boom perspective. Thus a supersonic regional jet (SSRJ) was chosen as a design example of the proposed multi-point design method. The design requirements and basic parameters of the SSRJ proposed by JAXA[19] were used as the baseline. The design requirements of this SSRJ are twin engines, 50 passengers, 3500nm range and cruise speed of M1.6. The basic parameters such as a wing area S_W and maximum take-off weight W_{TO} determined by the conceptual design study [19] are shown in Table 1. These parameters are used as the starting point of present multi-point optimizations. The take-off and landing field length requirement in this paper was set to 7,000 ft to make possible the use of conventional regional airports.

4.2 Phase One Design

4.2.1 Optimization of Wing Planform at Supersonic Cruise Condition

Wing planform optimization using iSIGHT-FD was carried out at the supersonic cruise condition of M1.6 and C_L=0.1 and at the same optimization conditions as described in section 3.2. The Pareto solution is shown in Fig. 9. The axes in this figure are the same as in Fig.8. Among all solutions which have drag less than 25 cts (drag counts, 1 ct=0.0001), three typical candidates were chosen: the planforms with the smallest drag (Type 1), the smallest bending moment (Type 2), and the smallest twisting moment (Type 3). Planforms of the selected three wings are shown in Fig.9(c). The details of warped wing sections of Type 2 are shown in Fig. 10 as an example, and its aerodynamic characteristics are shown in Fig. 11. This figure shows an example of a warp designed wing and its characteristics. By comparing the polar-curves of a flat plate wing and a warped wing (Fig.11(d)), it can be seen that the warped wing can reduce drag at some specified lift coefficients.

4.2.2 High-lift Device Design and Performance Estimation at Low Speed

QVLM-SA was used to design high-lift devices and estimate the aerodynamic performance at take-off and landing conditions. Three leading-edge flaps shapes with different area were considered. The three leading-edge flaps are named Flap A, B, C, where Flap A is the flap with smallest area, and Flap C is the flap with largest area. The outboard leading-edge flap is tapered and its chord length is 10% (Flap A), 20% (Flap B) and 30% (Flap C) of the local wing chord length. The inboard leading-edge flap is not tapered and its chord length is the same as the wing chord length at the wing kink location. Both the leading- and trailing-edge flaps are deflected by 10° downward when the angle is measured parallel to the free stream. The drag increment ΔC_D to the clean condition (no flap deflection) were calculated. The results for Type 2 are shown in Fig. 12. It can be seen that the flap shape with the largest area has the smallest ΔC_D. Due to the structural constraints, Flap B was selected.

4.2.3 Design of Tail-planes and the Area-Rule Fuselage

Next, other components such as tail-planes and the fuselage were designed. The tail planes were designed empirically based on past SST data [20]. Fuselage diameter and length were selected preliminary to be 7ft and 123ft, respectively, based on the consideration of cabin volume. According to the linear area rule theory, the area-ruled configurations with the same longitudinal distribution of cross-sectional area have the same wave drag for supersonic flows. The fuselage was then modified to have an equivalent cross-sectional area distribution of

Sears-Haack body, which has the minimum wave drag at supersonic conditions. Since the shapes of the main wing and tail planes have been designed, the necessary area distribution of the fuselage can be obtained by subtracting the area distributions of the wing and tail planes. In this design, the Sears-Haack Body area distribution was achieved by a T-tail layout (Fig. 13 for Type 2). Rear mount engine layout was also helpful to achieve the desired cross sectional area distribution. Longitudinal stability analysis was carried out by estimating locations of center of gravity, wing aerodynamic center, and tail-plane positions. It indicated a trim point without the use of elevators at supersonic cruise conditions.

4.2.4 Performance Comparisons of the Three Planform Types

The cruise performance of the designed aircraft are compared in Table 2. Since the three wing planform configurations selected have small difference in induced drag and all other components are common, only small differences were seen in cruise performance.

The take-off performance was calculated for three flap deflection cases by the method described in Ref. [21], which solved aircraft static force equation to estimate the take-off and landing performance. Three flap deflection cases considered are as follows.

- Case 1: no flap is deflected
- Case 2: only the trailing-edge flap is deflected by 10°
- Case 3: both leading- and trailing- edge flaps are deflected by 10°

Flap deflection angles were determined by conducting parametric studies of different flap deflection angles. The take-off field length (TOFL) and balanced field length (BFL) are compared in Table 3. It can be seen that Case 2 has the smallest BFL for every configuration. Though the LEF increases L/D by reducing the vortex lift and drag, the reduced lift will result in an increase in lift-off speed. Therefore, the case which generates the most lift (Case 2) will have the smallest lift-off speed and thus the smallest BFL. However, when considering the climb performance after take-off, the advantages will be different. The thrust-to-weight ratio T/W indicated in Table 4 are the necessary value to make an 8% climb at 250 kts. When comparing the T/W of the three cases, Case 3 has the smallest T/W. This is due to the large L/D achieved by the use of the leading-edge flap. A small T/W will result in reduction of engine noise, thus more environmental compatibility. Therefore, the flap deflection for configurations must be carefully considered to determine the BFL. In this design example, only the advantage of BFL was taken into account. A tolerance against the requirement of 7,000ft suggests the possibility to reduce the wing area further at phase two optimization.

4.3 Phase Two Design -Towards Optimization

Type 2 which has an advantage in structure, i.e. minimum bending moment M_x, was chosen to carry out the next design cycle as was shown in Fig. 1. The wing area was reduced to lessen the tolerance against the take-off field requirement. For simplicity, the wing planform was kept the same as that used in the first phase, and the weight reduction due to wing area reduction was considered (Since the cruise C_L will differ from that of the first phase due to reduction of aircraft weight, to obtain the true optimum, wing planform optimization using the new conditions is needed). Configurations and weights of all other components were also kept the same as those of the first phase. The profile drag was reduced because of the reduction of wing area, but the lift induced drag was increased. On the other hand, the necessary C_L was increased, which actually increased the L/D. The maximum weight of the aircraft was 133,500 lbs, which was lighter than the initial baseline. This weight was estimated by taking into account the fuel consumption using the mission fuel fraction method [13]. The BFL was increased and the tolerance against the requirement became smaller. The comparison of performance of the first and second phase configurations are shown in Table 5, and the aircraft configuration is shown in Fig. 14. Since there is still a tolerance against the BFL requirement, a possibility is left for further improvement.

5 Some Limitations and Challenges

It can be said from the above design example that, the multi-point design method presented in this paper can consider both low-speed and supersonic flight conditions; furthermore, it is possible to improve cruise performance, reduce wing area and thus aircraft weight. However there remain some limitations in the design. Firstly, the wing planform optimization was carried out to minimize only the lift-induced drag, but when considering the cruise performance of the entire aircraft, wave and parasite drag must be included in the drag minimization because the wave drag might cancel out the advantage of induced drag. Secondly, this multi-point design does not take into account the level of sonic boom. The sonic boom is one of the large problems to realize the SST, and a SST without installing low sonic boom technologies will most likely not be certified to fly over land.

Nevertheless, it is not easy to bring wave drag, parasite drag and sonic boom into this optimization design process. These factors depend strongly on the entire aircraft configuration, and in order to optimize the tail-plane design and trim analysis will need to be automated. In the current situation, tail-plane planform design / positioning and Area-Rule fuselage design are done manually, while analyzing the longitudinal stability. There are many parameters to be determined, and it is up to the designer to decide whether the aircraft configuration is acceptable. For these reasons, further research will be needed for a complete automatic design process, which is necessary for integrated design optimization.

Also, the trim drag is not considered in the proposed method, because there are difficulties in obtaining the aerodynamic pitching moment due to the leading-edge separation vortex. It is required to assume the location of the vortex. Trim drag will possibly reduce the *L/D* and the performance.

Furthermore, the weight estimation method used in this study is based on empirical and low-fidelity methods. Therefore, a thorough optimization of wing area, thus aircraft weight is impossible. In other words, the optimum obtained by this method will not be a reliable optimum. So, the proposed method should be used as a guideline which will indicate a direction of optimization.

6 Conclusions

In this paper, a multi-point design method for the SST which considers both low-speed and supersonic performance was proposed.

(1) A low fidelity method to estimate low-speed aerodynamic performance was developed by coupling the Quasi-Vortex-Lattice Method and the Leading-Edge Suction Analogy (QVLM-SA). The calculation results of QVLM-SA were compared with wind-tunnel test results, and comparisons show that the QVLM-SA can reproduce the experiment well at low angles of attack. Also flap effects were compared between experiment and calculation, and the results show that QVLM-SA is capable of estimating effects of flaps qualitatively.

(2) By using the supersonic linear theory and the Carlson's warp design method with a commercially-available software iSIGHT-FD, wing planforms were optimized at supersonic cruise conditions. Structural characteristics were also calculated to avoid structurally-unrealistic wing shapes. Preliminary calculations were carried out using iSIGHT-FD and results showed that there was a trade-off between aerodynamic performance and structure.

(3) A multi-point design process was proposed. It employs wing optimization at supersonic speeds and high-lift device design at low-speeds. The example design of a SSRJ showed that by the use of this design process, it is possible to design a supersonic aircraft with less weight and improved aerodynamic performance

Acknowledgement

The authors would like to thank Dr. Yoshida of the Japan Aerospace Exploration Agency for his beneficial advice and assistance in computational matters and SST design.

References

[1] Aronstein, D.C. and Schueler, K.L., "Two Supersonic Business Aircraft Conceptual Designs With and Without Sonic Boom Constraint," *Journal of Aircraft*, Vol.42, No.9, 2005, pp.775-786.

[2] Henne, P., "Case for Small Supersonic Civil Aircraft," *Journal of Aircraft*, Vol.42, No.9, 2005, pp.765-774.

[3] "HISAC, Environmentally Friendly High Speed Aircraft Project," http://www.hisacproject.com/ [retrieved 28 April 2008].

[4] Onuki, T., Hirako, K. and Sakata, K., "National Experimental Supersonic Transport Project," *the 25th Congress of the International Council of the Aeronautical Sciences*, ICAS 2006-1.4.1, Hamburg, 2006.

[5] Murakami, A., "Silent Supersonic Technology Demonstration Program," *the 25th Congress of the International Council of the Aeronautical Sciences*, ICAS 2006-1.4.2, Hamburg, 2006.

[6] Lan, C. E., "A Quasi-Vortex-Lattice Method in Thin Wing Theory," *Journal of Aircraft*, Vol.11, No.9, 1974, pp. 518-527.

[7] Polhamus, E. C., "A Concept of the Vortex Lift of Sharp-Edge Delta Wings Based on a Leading-Edge Suction Analogy," NASA TN D-3767, 1966.

[8] Carlson, H. W., and Miller, D. S., "Numerical Methods for the Design and Analysis of Wings at Supersonic Speeds," NASA TN D-7731, 1974.

[9] Higuchi K., Rinoie, K., Lei, Z., and Kwak D., "A Low Fidelity Method for Flap Aerodynamic Design of a Cranked- Arrow Wing," *25th AIAA Applied Aerodynamics Conference*, AIAA Paper 2007-4178, Miami, 2007.

[10] Yoshida, K., "Overview of NAL's Program Including the Aerodynamic Design of the Scaled Supersonic Airplane," held at the VKI, RTO Educational Notes 4, 15-1~16, 1998.

[11] Kanno, Y., Iwasaki, K., "Stuctural Weight Estimation for Winged Vehicles (in Japanese)," National Aerospace Laboratory Technical Report, NAL TR-1351, 1997.

[12] Harloff, G. J., and Berkowitz, B. M., "HASA—Hypersonic Aerospace Sizing Analysis for the Preliminary Design of Aerospace Vehicles," NASA CR-182226, 1988.

[13] Raymer, D. P., Aircraft Design: A Conceptual Approach (AIAA education series) Second Edition, American Institute of Aeronautics and Astronautics, Inc., Washington, D.C., 1992.

[14] Kwak, D., Miyata, K., Noguchi, M., Sunada, Y. and Rinoie, K., "Experimental Investigation of High Lift Device for SST (in Japanese)," National Aerospace Laboratory Technical Report, NAL TR-1450, 2002.

[15] Rinoie, K., Miyata, K., Kwak, D.Y. and Noguchi, M., "Studies on Vortex Flaps with Rounded Leading-Edges for Supersonic Transport Configuration," *Journal Aircraft*, Vol.41, No.4, pp.829-838, 2004.

[16] Jorgensen, L. H., "Prediction of Static Aerodynamic Characteristics for Space-Shuttle-Like and Other Bodies at Angles of Attack from 0° to 180°," NASA TN D-6996, 1973.

[17] Quinto, P. F., Paulson, J. W. Jr., "Flap Effectiveness on Subsonic Longitudinal Aerodynamic Characteristics of a Modified Arrow Wing," NASA TM-84582, 1983.

[18] Coe, P. L., Jr., Kjelgaard, S. O., and Gentry, G. L., Jr., "Low-Speed Aerodynamic Characteristics of a Highly Swept, Untwisted, Uncambered Arrow Wing," NASA TP-2176, 1983.

[19] Horinouchi. S., "Future of the Next Generation Supersonic Airplane (in Japanese)," *Journal for Japan Society of Fluid Mechanics*, Vol.25, pp. 337-344, 2006.

[20] Roskam, J., Airplane Design Part II: Preliminary Configuration Design and Integration of the Propulsion System, DAR Corporation, Lawrence, Kansas, 1997.

[21] Miyata, K. and Rinoie, K., "Estimation of Take-off Performance for Supersonic Transport with Leading-edge Vortex Flaps and Trailing-edge Flaps (in Japanese)," *Journal of the Japan Society for Aeronautical and Space Sciences*, Vol.51, No.593, pp.327-329, 2003

Appendix A Optimization Algorithm

Two types of genetic algorithms (GA) were used in this paper. One is the Multi-Island Genetic Algorithm (MIGA), and the other is the Neighbor Cultivation Genetic Algorithm (NCGA). These optimization methods are included in the commercially available optimization software iSIGHT-FD.

MIGA distributes the individuals to different groups (islands) and genetic search is performed on the islands independently. However, at some probability individuals will migrate to other islands. This method was developed to avoid localized solutions as well as improving performance.

NCGA is a powerful multi-objective genetic algorithm which uses neighborhood crossover. To obtain a Pareto solution in a multi-objective optimization, the algorithm will need to search globally to obtain a broad range of solutions. On the other hand, a local search must be done to ensure the solutions are accurate. There are common techniques for a

global search which is used among many algorithms. However, these algorithms cannot perform sufficient local search. NCGA uses crossovers between individuals which are close in the objective function space to carry out a sufficient local search.

Copyright Statement

Table 1. Basic parameters of JAXA's SSRJ[19].

Wing area	1,883 ft^2
Maximum weight	144,000 lb
Thrust per engine	31,000 lb
Design C_L	0.1

Table 2. Comparison of drag and L/D at supersonic cruise for the three planform types.

	Type 1	Type 2	Type 3
Induced drag	0.00226	0.00248	0.00250
Wave drag	0.00392	0.00363	0.00357
Parasite drag	0.00750	0.00744	0.00745
Total	0.0136	0.01355	0.01347
Cruise lift-to-drag ratio C_L=0.1	7.30	7.38	7.40

Table 3. Comparison of take-off field length for the three planform types and three flap deflection cases.

	Type 1	Type 2	Type 3
Case 1			
TOFL	5495	5884	6072
BFL	6562	7051	7290
Case 2			
TOFL	4698	4972	5181
BFL	5591	5934	6196
Case 3			
TOFL	5246	5562	5819
BFL	6275	6675	7005

Table 4. Comparison of L/D and necessary T/W for an 8%, 250 kt climb for the three planform types and three flap deflection cases.

	Type 1	Type 2	Type 3
Case 1			
L/D	5.60	5.29	5.20
T/W	0.258	0.268	0.272
Case 2			
L/D	6.52	6.13	5.95
T/W	0.233	0.243	0.248
Case 3			
L/D	10.1	8.97	8.66
T/W	0.179	0.191	0.195

Table 5. Comparison of characteristics of phase 1 and 2 configurations.

	Phase One	Phase Two
Maximum weight [lb]	144,000	133,500
Wing weight [lb]	8,958	7,578
Wing area [ft^2]	1,883	1,530
Cruise C_L	0.1	0.11
Induced drag	0.00248	0.00300
Wave drag	0.00363	0.00379
Parasite drag	0.00744	0.00689
L/D	7.38	8.04
Balanced field length [ft]	5934	6391
Necessary Thrust for climb [lb]	27515	25220
Landing Field Length [ft]	4241	4896

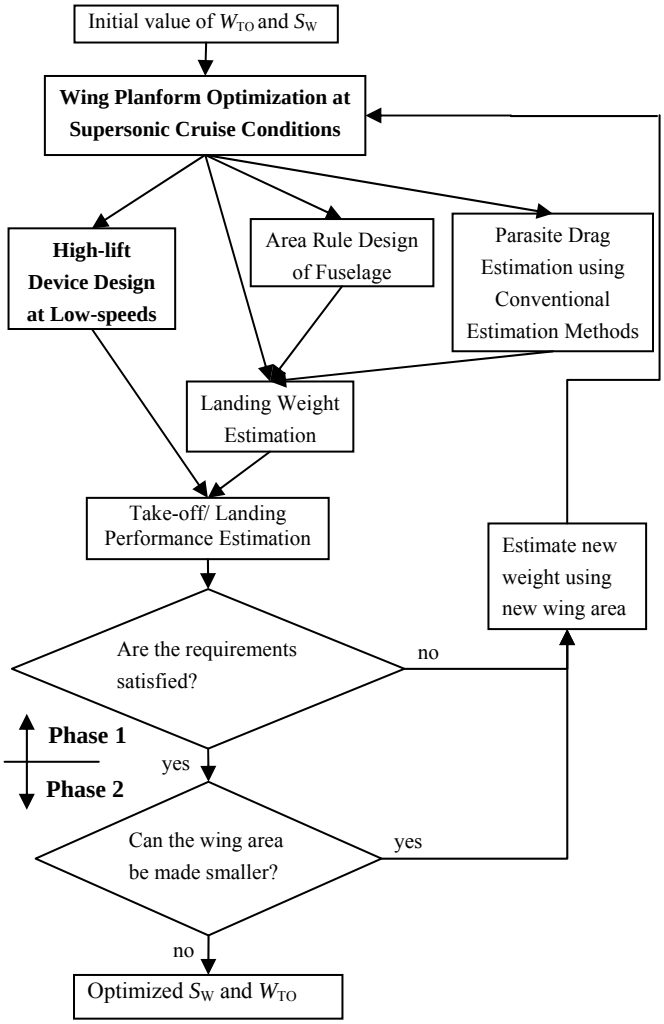

Fig. 1. Multi-point Design Method.

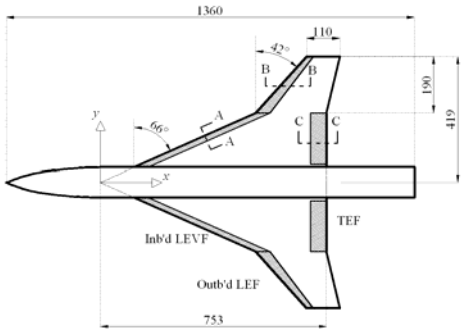

Fig. 2. NAL Wind-tunnel Test Model Dimensions (unit: mm).

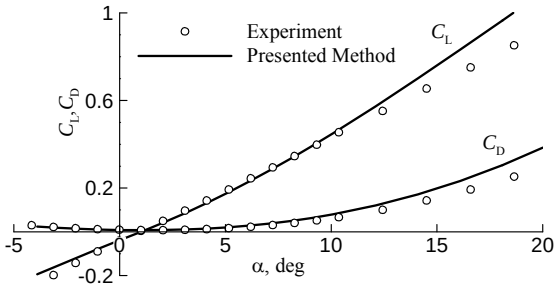

(a) S000000

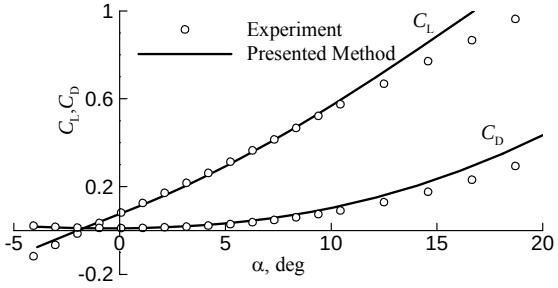

(b) S000010

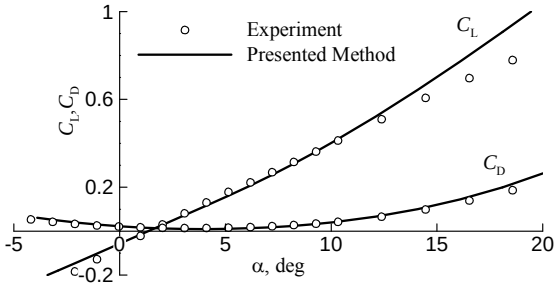

(c) S301200

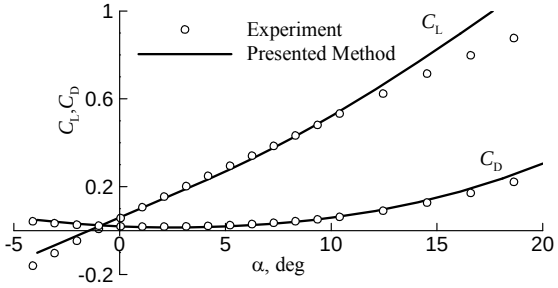

(d) S301210

Fig. 3. Comparison of experiment and calculation for S000000, S000010, S301200, and S301210.

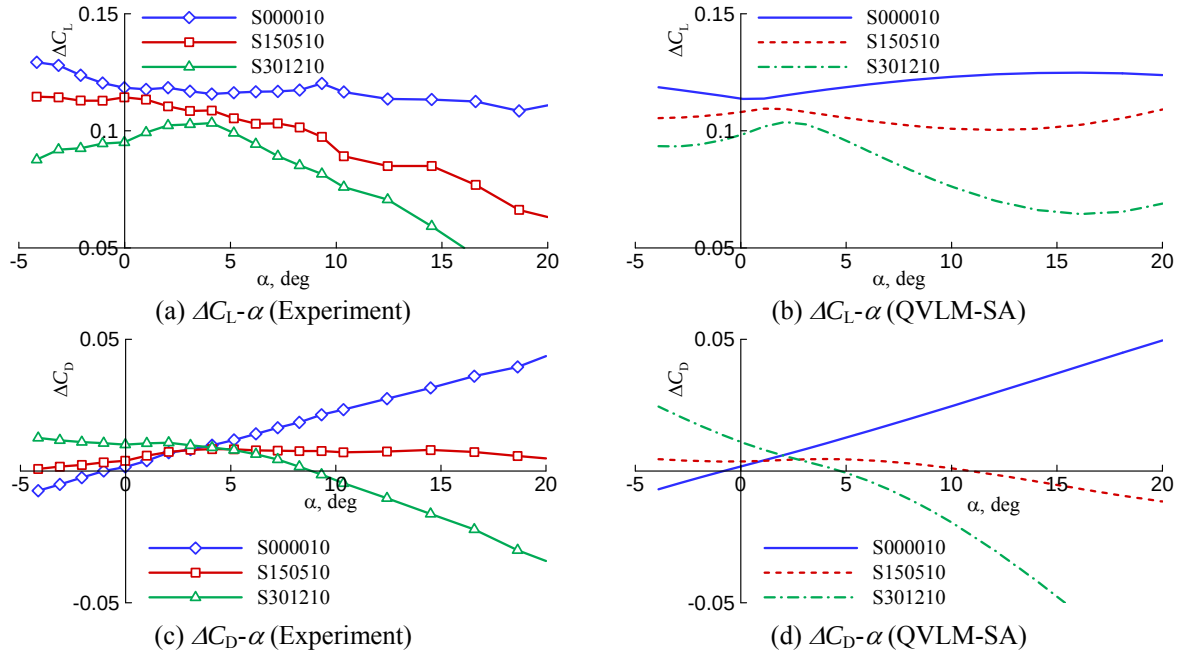

(a) ΔC_L-α (Experiment) (b) ΔC_L-α (QVLM-SA)

(c) ΔC_D-α (Experiment) (d) ΔC_D-α (QVLM-SA)

Fig. 4. Lift and drag increments (ΔC_L, ΔC_D) of S000010, S150510, S301210.

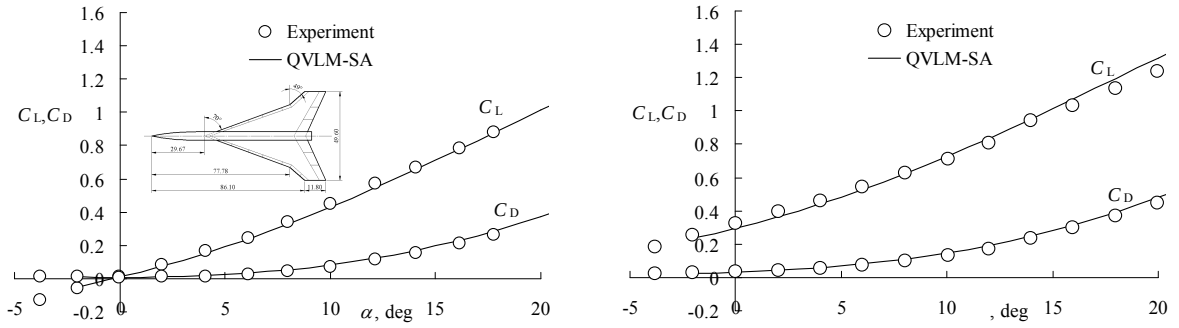

(a) without flap deflections (b) δ_{le}= 10deg (6 segments) δ_{te}=20deg (3 segments)

Fig. 5. Comparison of experiment by Quinto et al.and calculation (QVLM-SA).

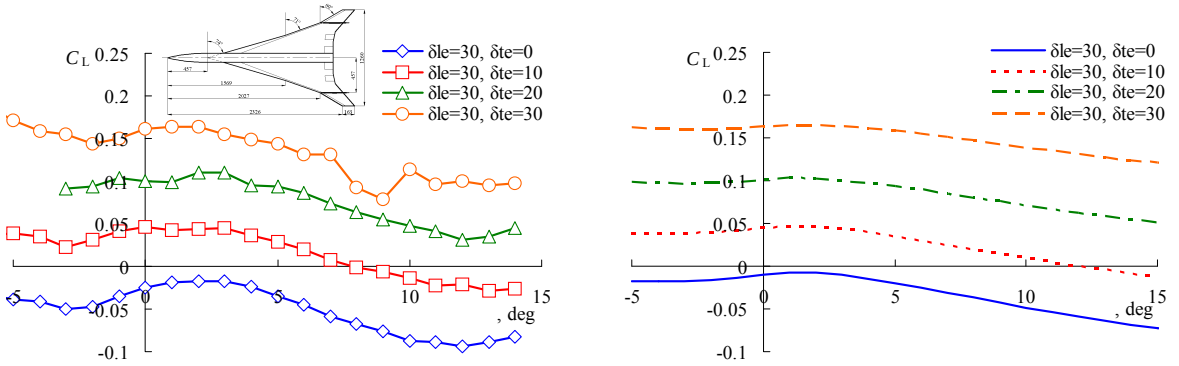

(a) ΔC_L-α (Experiment) (b) ΔC_L-α (Calculation)

Fig. 6. Comparison of experiment by Coe al.and calculation (QVLM-SA).

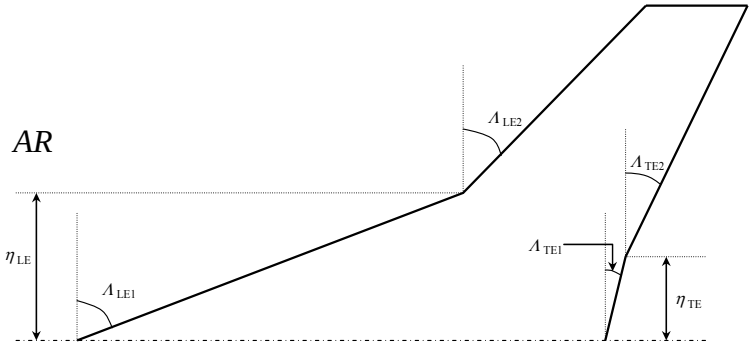

Fig. 7. Design parameters of the cranked arrow wing.

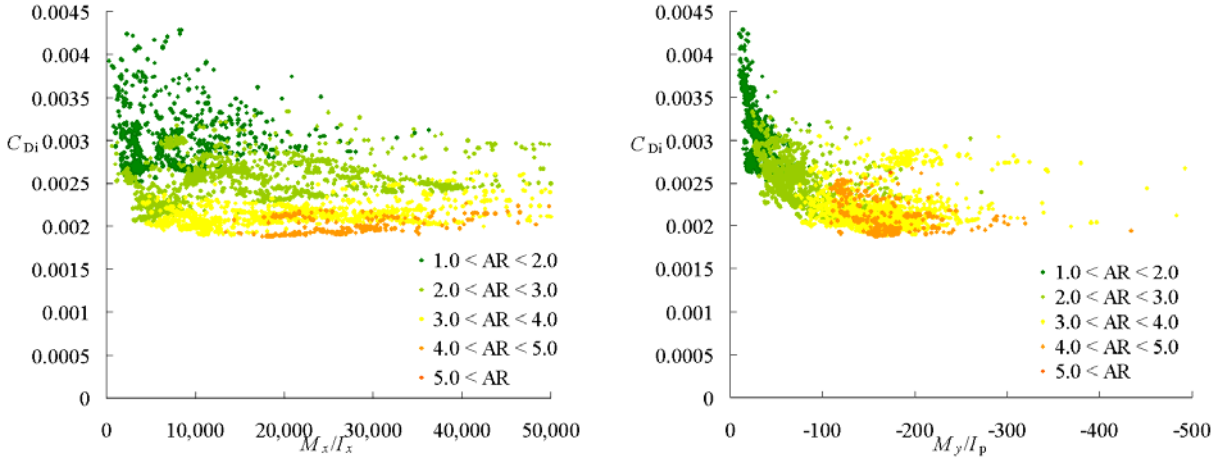

(a) Induced drag versus bending moment. (b) Induced drag versus twisting moment.

Fig. 8. Results of the preliminary iSIGHT-FD calculation.

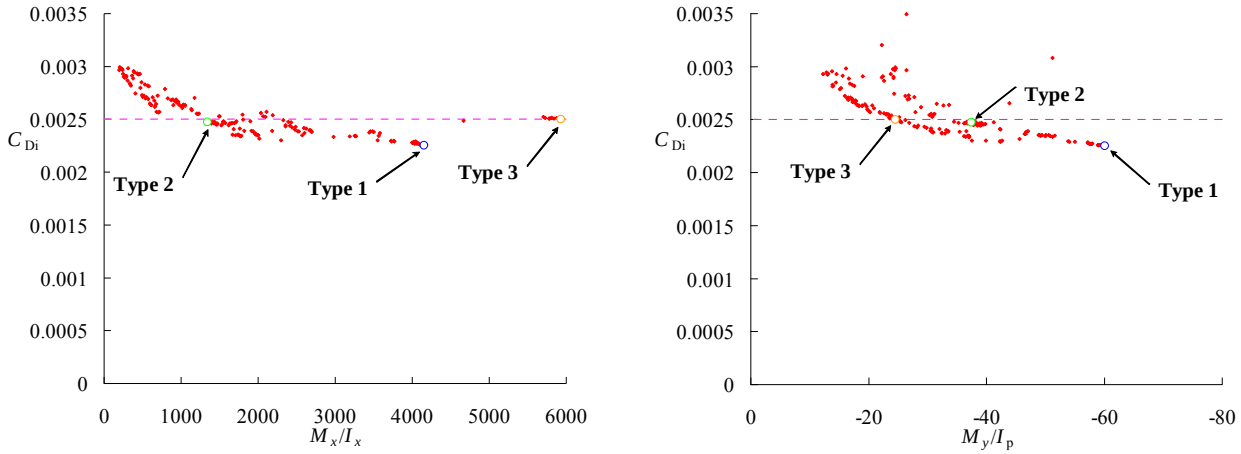

(a) Induced drag versus bending moment. (b) Induced drag versus twisting moment.

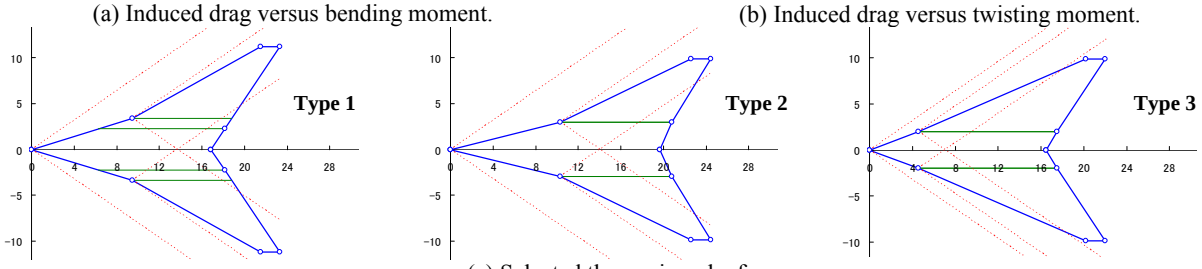

(c) Selected three wing planforms

Fig. 9. Pareto solution of the optimization calculation.

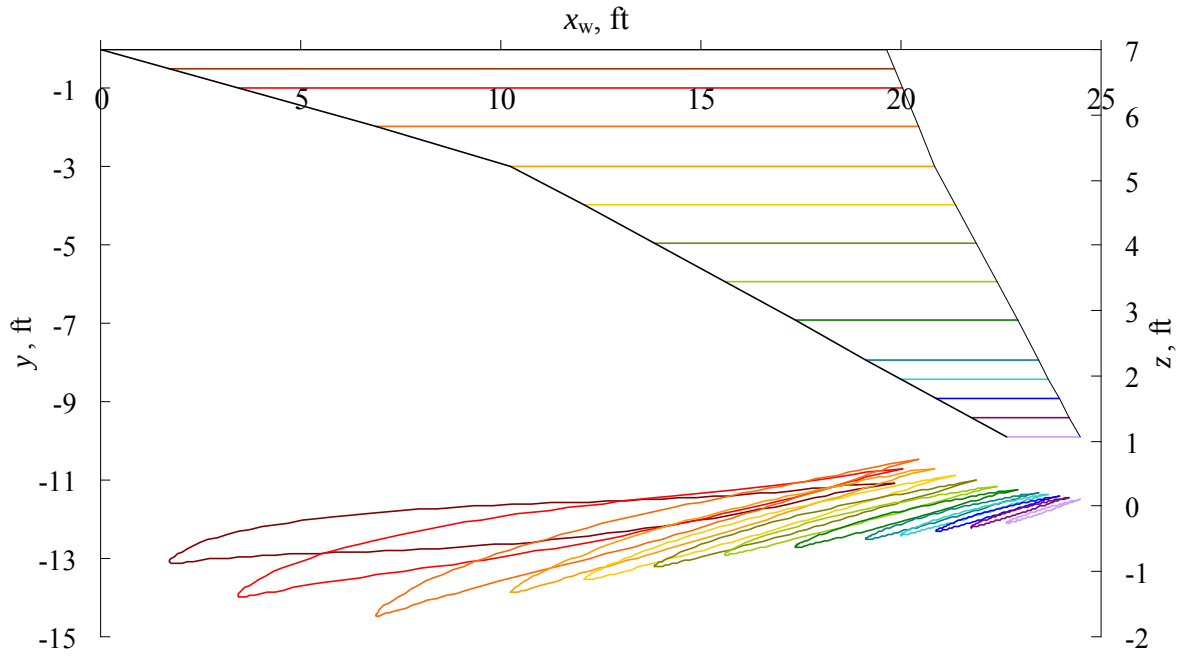

Fig. 10. Warped wing section of Type 2.

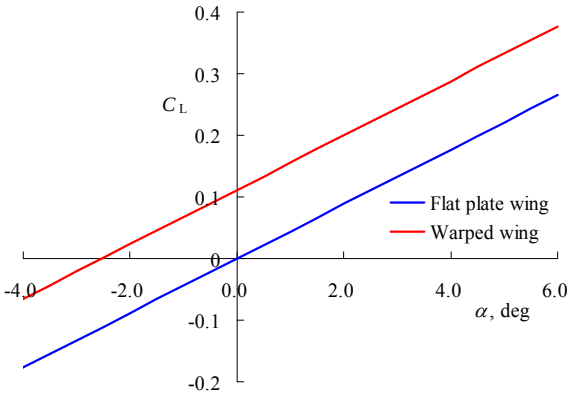

(a) C_L-α curve

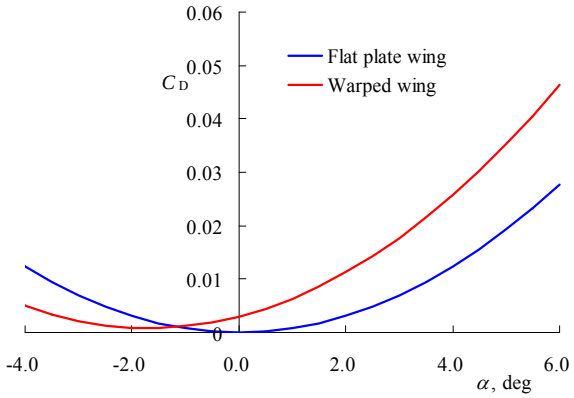

(b) C_D-α curve

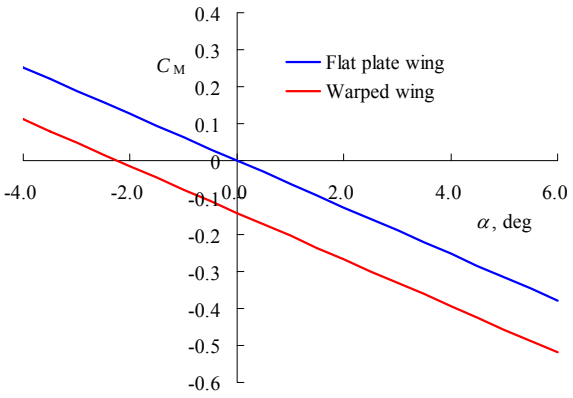

(c) C_M-α curve

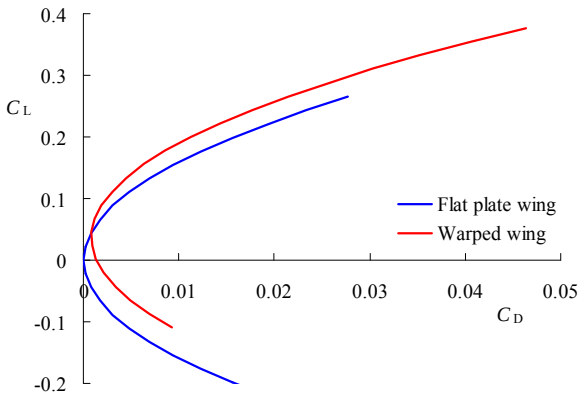

(d) C_L- C_D curve

Fig. 11. Aerodynamic characteristics of Type 2.

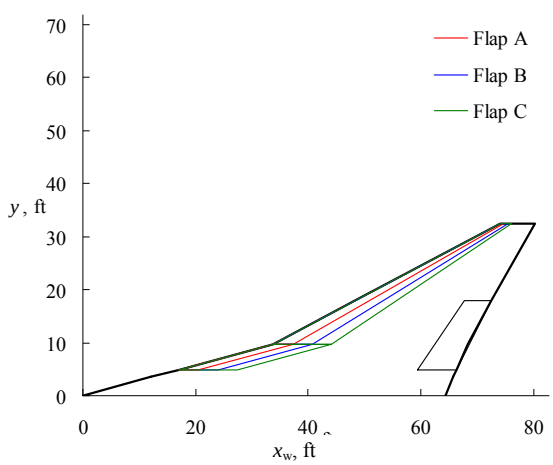

(a) Leading-edge flap shapes.

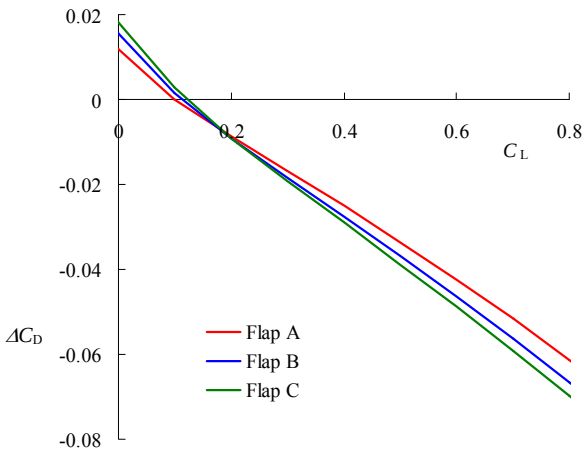

(b) ΔC_D versus C_L curve.

Fig. 12 . Comparison of leading-edge flap shapes for wing planform Type 2.

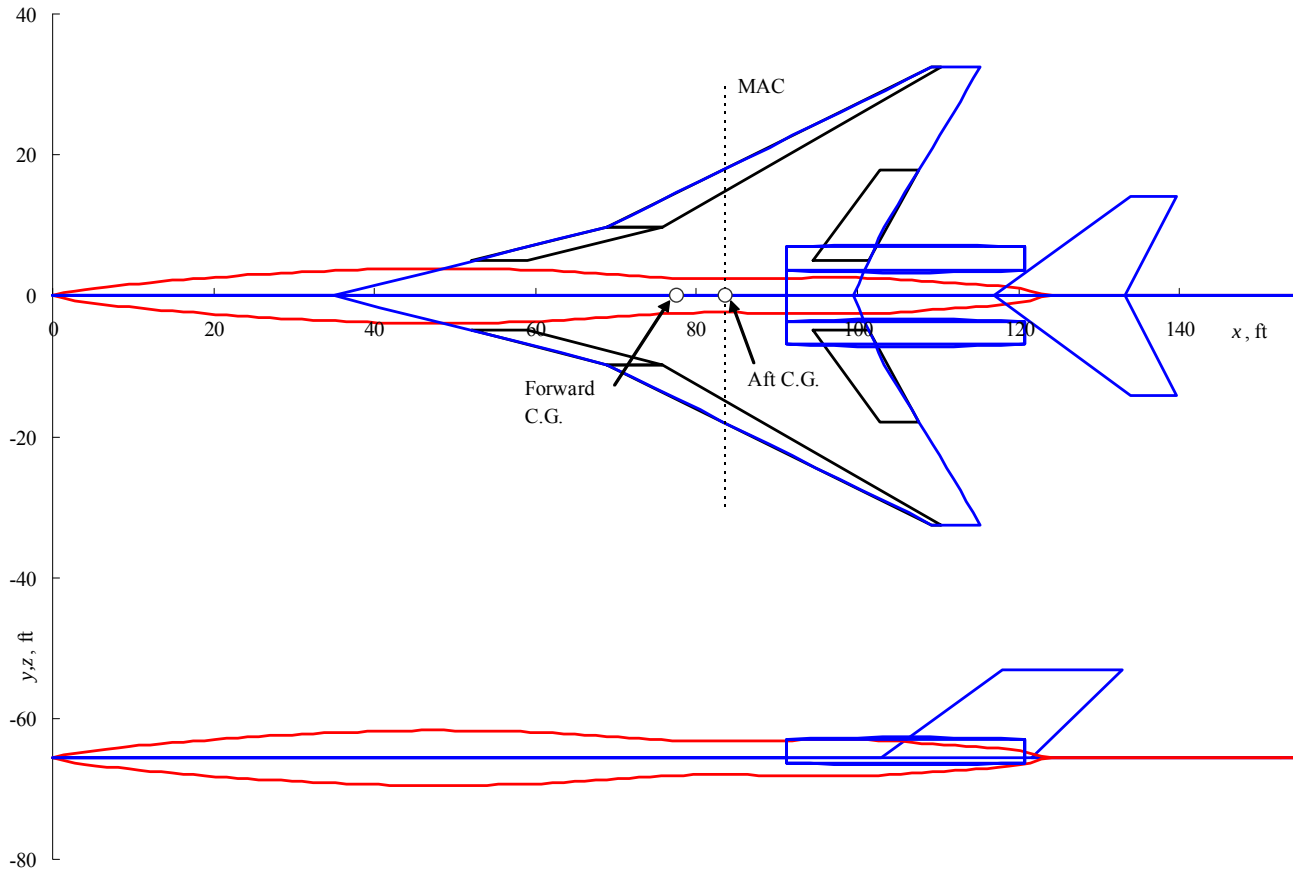

Fig. 13. Result of Area-Rule fuselage design for Type 2.

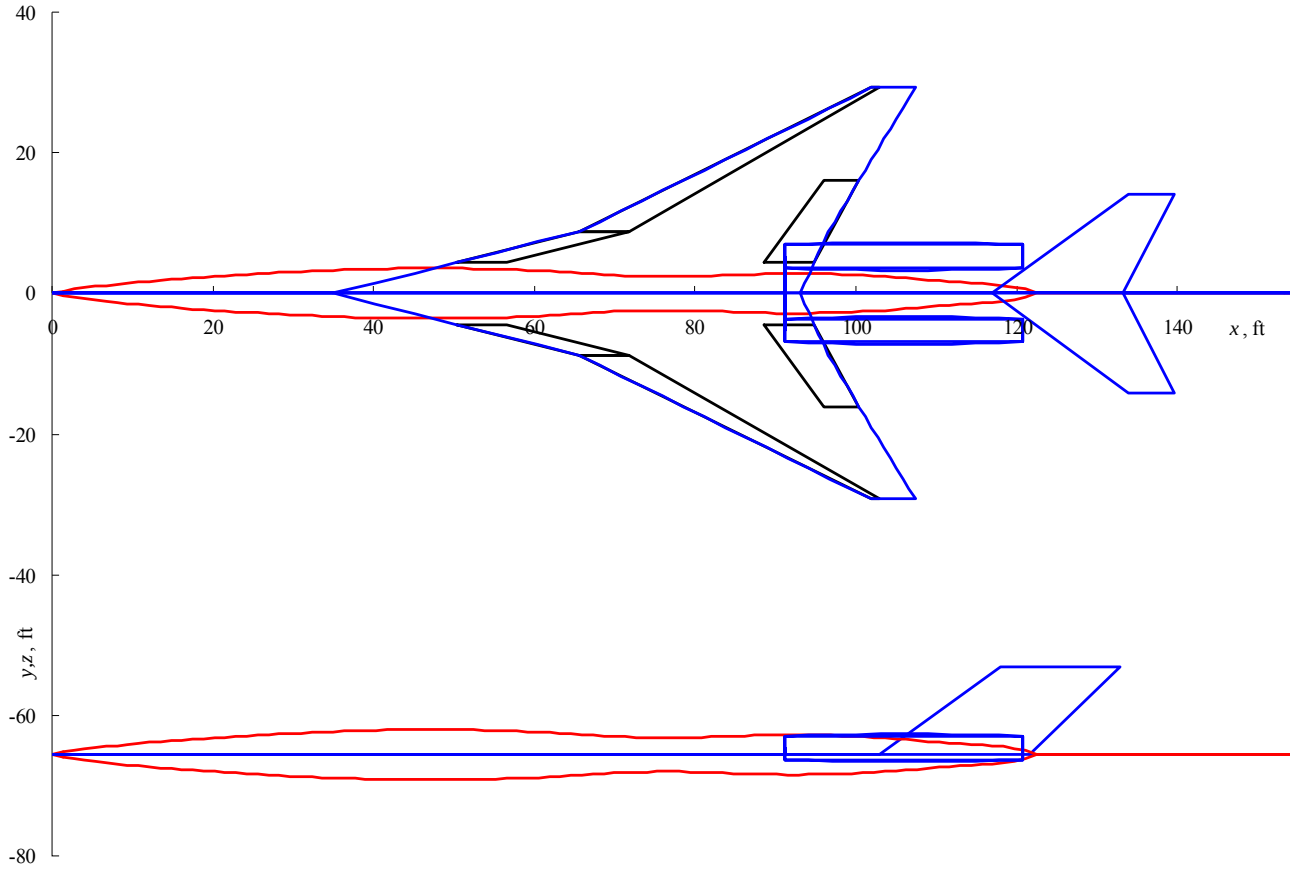

Fig. 14. Second phase configuration of Type 2.